

Control system of the grid-connected converter based on a state current regulator with oscillatory terms

Abstract. This paper presents a state-feedback current controller with oscillatory terms for three-phase grid-connected PWM converters. Use of the oscillatory terms allows for shaping the sinusoidal input currents of the converter under distorted grid voltage conditions. Linear-quadratic optimization method is used to calculate the current controller gains. In the converter control structure the state current controller and PI DC-link voltage controller are used. Mathematical analysis and simulation results of the proposed control system are presented and discussed.

Streszczenie. W artykule przedstawiono regulator prądu ze sprzężeniem od wektora stanu z rozszerzeniem o człony oscylacyjne opracowany dla trójfazowych przekształtników sieciowych PWM. Wykorzystanie członów oscylacyjnych pozwala na kształtowanie sinusoidalnego prądu wejściowego prostownika przy odkształconym napięciu sieci. Współczynniki wzmacnień regulatora prądu obliczono z wykorzystaniem optymalizacji liniowo-kwadratowej. W strukturze sterowania przekształtnikiem zastosowano opracowany regulator prądu oraz regulator PI napięcia DC-linku. Przedstawiono analizę matematyczną i omówiono wyniki badań symulacyjnych. (Układ sterowania przekształtnikiem sieciowym wykorzystujący regulator stanu ze sprzężeniem od prądów i sygnałów z członów oscylacyjnych)

Keywords: grid-connected converter, linear-quadratic regulator, current controller, harmonic distortion

Słowa kluczowe: przekształtnik sieciowy, regulator liniowo-kwadratowy, regulator prądu, odkształcenie wyższymi harmonicznymi

Introduction

Three-phase grid-connected voltage source converters (VSCs) are reliably used in a wide diversity of industrial applications such as adjustable speed drives [1], renewable energy systems [2], [3], power conditioning systems [4] or vehicle-to-grid systems [5]. The conventional control strategies [6] like voltage oriented control (VOC) or direct power control (DPC) are widely used for DC-link voltage regulation, bidirectional power flow control, power factor correction and for shaping nearly sinusoidal converter input currents. These strategies were designed to control only the fundamental component of the current. However, the power quality problems, such as a harmonic pollution, were marginal through the years when these methods were developed.

Nowadays, the power quality problems are escalating, primarily due to an increasing number of nonlinear and unbalanced loads connected to the power system. Grid voltage distortions can cause problems in control of grid-connected converters, such as distorted and asymmetric AC currents, dc-link voltage oscillations. Therefore, many of the control strategies have been proposed for VSC converters operating under the distorted grid conditions. In the case of grid voltage asymmetry, symmetrical components strategy has been widely used, e.g. [7]. In order to obtain the sinusoidal grid currents under the distorted grid voltage, a multireference frame system has been proposed [8]. The harmonics are transferred to DC signals and then proportional-integral (PI) or integral controllers are used to reduce these current components. Other popular solutions are based on proportional-resonant (PR) controllers in the rotating [9] or the stationary frame [10]. The latter solutions involve predictive controllers [11], [12], flatness based controllers [13] or repetitive controllers [14]. A different approach using a state-space technique is presented in [15] and [16] for the grid-connected PWM converter with LCL filter based on the pole placement method. However, knowledge about the proper location of the closed-loop poles is required. It is helpful to use a linear-quadratic (LQ) optimization method to calculate the state feedback matrix gain for a system, for example, like in [17] and [18]. An LQ controller with the oscillatory term is used [19], [20], [21] for the constant-amplitude constant-frequency sine wave inverters in previous work.

In this paper a state feedback current controller with

the oscillatory terms for the three-phase three-wire grid-connected converter is presented. The main features of using the oscillatory terms is to obtain sinusoidal symmetrical grid currents under distorted grid voltage conditions. The 5th, 7th, 11th and 13th harmonics of the grid voltage have usually the largest amplitudes and the L filter has the weakest attenuation for these harmonics. Therefore, the high order harmonic current compensation is applied to 13th. Balancing of the grid currents under unbalanced grid voltage is one of the frequently proposed approaches [22]. However, some researches argue that the grid voltage imbalance should not be modified by control from the point of view of the grid [23]. In this paper both strategies are considered. The converter control system has been designed using VOC method. In order to track space vector grid-voltage angle the 3-phase lock-loop, based on rotating reference frame, (PLL block) is used [24]. In the outer DC-link voltage control loop, the PI controller with an anti-windup is used. The proposed control strategy (Fig. 2) for three-phase grid-connected PWM converter (Fig. 1) has been verified in a simulation using Matlab/Simulink environment.

System description

The two-level three-phase grid-connected PWM converter is shown in Fig. 1. It is connected through an inductance filter to the grid. The R , L and C_{dc} are the resistance and the inductance of the phase filter legs and the DC-link capacitance, respectively. The converter is loaded by the R_{load} .

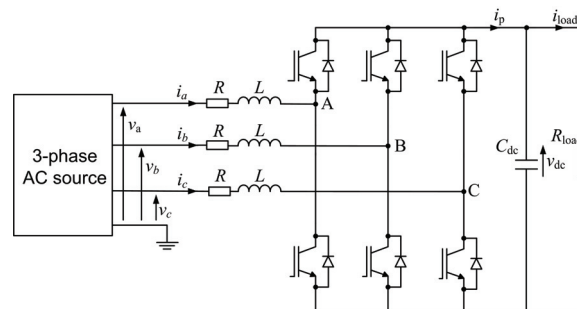


Fig. 1. Three-phase grid-connected PWM converter

The average model of a three-phase active rectifier in dq coordinates is expressed by (1) to (3) obtained using state-

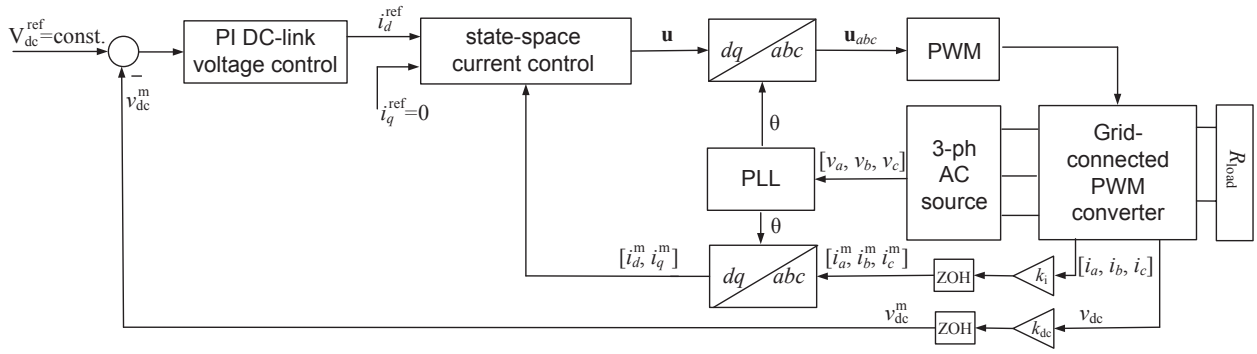


Fig. 2. Block diagram of the converter control structure

space average technique [18]. In the presented approach it is assumed that the v_d and v_q are an ideal three-phase grid voltage source in dq frame and v_{dc} is an ideal DC-link voltage source. Thus:

$$(1) \quad \frac{d}{dt} i_d = -\frac{R}{L} i_d - \frac{1}{L} v_{dc} d_d + \omega i_q + \frac{1}{L} v_d,$$

$$(2) \quad \frac{d}{dt} i_q = -\frac{R}{L} i_q - \frac{1}{L} v_{dc} d_q - \omega i_d + \frac{1}{L} v_q,$$

$$(3) \quad \frac{d}{dt} v_{dc} = \frac{1}{C_{dc}} \left(\frac{3}{2} d_d i_d + \frac{3}{2} d_q i_q - i_{load} \right).$$

The converter model given by (1) to (3) is nonlinear because of the product of the duty cycles d_d , d_q and the grid currents i_d , i_q or v_{dc} , respectively. The linear model, on the other hand, is required for the linear control design. The small-signal linearization technique is widely used in such cases [25]. For the state current controller design only the two current equations (1) and (2) are used. This way the linearization problem can be reduced assuming that v_{dc} is V_{dc} .

State-space model for the current control design

The state-space model with physical state vector of the plant for current control design is given by (4). The grid current measurement gain k_i is incorporated into this model:

$$(4) \quad \frac{d}{dt} \mathbf{x} = \mathbf{A} \mathbf{x} + \mathbf{B} \mathbf{u} + \mathbf{E} \mathbf{v},$$

where:

$$(5) \quad \mathbf{A} = \begin{bmatrix} -\frac{R}{L} & \omega \\ \omega & -\frac{R}{L} \end{bmatrix}, \quad \mathbf{x} = \begin{bmatrix} i_d^m \\ i_q^m \end{bmatrix},$$

$$(6) \quad \mathbf{B} = \begin{bmatrix} -\frac{V_{dc}}{L} k_i & 0 \\ 0 & -\frac{V_{dc}}{L} k_i \end{bmatrix}, \quad \mathbf{u} = \begin{bmatrix} d_d \\ d_q \end{bmatrix},$$

$$(7) \quad \mathbf{E} = \begin{bmatrix} \frac{1}{L} k_i & 0 \\ 0 & \frac{1}{L} k_i \end{bmatrix}, \quad \mathbf{v} = \begin{bmatrix} v_d \\ v_q \end{bmatrix}.$$

There are two measurement grid currents i_d^m and i_q^m , which are state variables, the two duty cycles d_d and d_q as inputs, and two grid voltages v_d and v_q as the disturbances collected in the \mathbf{x} , \mathbf{u} and \mathbf{v} vectors and the three matrices: \mathbf{A} – the state matrix, \mathbf{B} – the control matrix and \mathbf{E} – the disturbance matrix. The output equation is defined as follows: $\mathbf{y} = \mathbf{C} \mathbf{x}$, where \mathbf{C} is the identity matrix.

In order to minimize steady-state error $i_x^m - i_x^{\text{ref}}$ under constant disturbances, the plant is augmented by integral terms (8). Therefore, the state vector is augmented by a \mathbf{p} part consisting of p_d and p_q .

$$(8) \quad \frac{d}{dt} p_x = i_x^m - i_x^{\text{ref}},$$

where subscript $x = \{d, q\}$.

Similarly, in order to minimize a sinusoidal component of steady-state error $i_x^m - i_x^{\text{ref}}$, the plant is augmented by oscillatory terms [9]. One oscillatory term is described by (9).

$$(9) \quad \frac{d}{dt} r_{1x} = r_{2x}, \quad \frac{d}{dt} r_{2x} = i_x^m - i_x^{\text{ref}} - (h\omega)^2 r_{1x},$$

where subscript $x = \{d, q\}$ and h is the number of compensated pulsation in error current signal.

The state-space model with the state vector augmented by the auxiliary state variables collected in the \mathbf{p} vector (integral part) and the auxiliary state variables collected in the \mathbf{r} vector (oscillatory part) is given in (10). In the abc frame, fifteen oscillatory terms are needed for the 5th, 7th, 11th and 13th harmonic compensation and for current balancing. After dq transformations 5th and 7th harmonics become 6th harmonic component and both can be compensated by a single oscillatory term. Similarly, 11th and 13th harmonics become 12th harmonic. The grid voltage imbalance causes the 2nd harmonic in the i_d and i_q . Finally, six oscillatory terms are implemented. Therefore

$$(10) \quad \frac{d}{dt} \mathbf{x}_{\text{aug}} = \mathbf{A}_{\text{aug}} \mathbf{x}_{\text{aug}} + \mathbf{B}_{\text{aug}} \mathbf{u} + \mathbf{E}_{\text{aug}} \mathbf{v},$$

where:

$$(11) \quad \mathbf{A}_{\text{aug}} = \begin{bmatrix} \mathbf{A} & \mathbf{0} \\ \mathbf{I} & \mathbf{0} \\ \mathbf{0} & \mathbf{0} & \mathbf{0} & \mathbf{I} & \mathbf{0} & \mathbf{0} & \mathbf{0} & \mathbf{0} \\ \mathbf{I} & \mathbf{0} & \mathbf{W}_2 & \mathbf{0} & \mathbf{0} & \mathbf{0} & \mathbf{0} & \mathbf{0} \\ \mathbf{0} & \mathbf{0} & \mathbf{0} & \mathbf{0} & \mathbf{0} & \mathbf{I} & \mathbf{0} & \mathbf{0} \\ \mathbf{I} & \mathbf{0} & \mathbf{0} & \mathbf{0} & \mathbf{W}_6 & \mathbf{0} & \mathbf{0} & \mathbf{0} \\ \mathbf{0} & \mathbf{I} \\ \mathbf{I} & \mathbf{0} & \mathbf{0} & \mathbf{0} & \mathbf{0} & \mathbf{0} & \mathbf{W}_{12} & \mathbf{0} \end{bmatrix},$$

$$(12) \quad \mathbf{x}_{\text{aug}} = \begin{bmatrix} \mathbf{x} \\ \mathbf{p} \\ \mathbf{r} \end{bmatrix}, \quad \mathbf{B}_{\text{aug}} = \begin{bmatrix} \mathbf{B} \\ \mathbf{0} \end{bmatrix}, \quad \mathbf{E}_{\text{aug}} = \begin{bmatrix} \mathbf{E} \\ \mathbf{0} \end{bmatrix},$$

then

$$(13) \quad \mathbf{W}_h = -\text{diag}([(h\omega)^2, (h\omega)^2]),$$

and $h = \{2, 6, 12\}$.

There are augmented matrices: \mathbf{A}_{aug} – the augmented state matrix, \mathbf{B}_{aug} – the augmented control matrix, \mathbf{E}_{aug} – the augmented disturbance matrix. The \mathbf{x}_{aug} , \mathbf{u} , and \mathbf{v} are represents respectively the new augmented state, the control and the disturbance vectors.

An LQ current controller with oscillatory terms design

The current control structure with full-state-feedback is presented in Fig. 3.

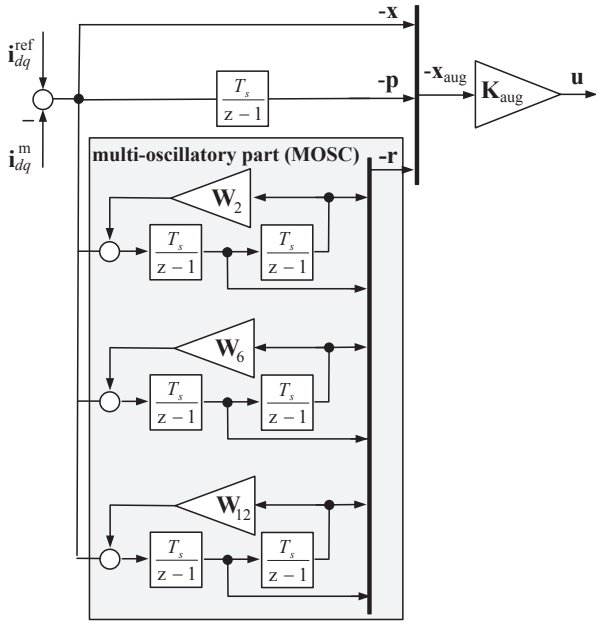


Fig. 3. Block diagram of the current control structure

For this purpose, the LQ method in the discrete time domain is applied using `lqrd` Matlab's function. Firstly, the continuous-time model is discretized. Next, the state-feedback matrix \mathbf{K}_{aug} is calculated according to the discrete state-feedback law:

$$(14) \quad \mathbf{u}(k) = -\mathbf{K}_{\text{aug}}\mathbf{x}_{\text{aug}}(k),$$

minimizes a discrete cost function:

$$(15) \quad J = \sum_{k=0}^{\infty} (\mathbf{x}_{\text{aug}}^T(k)\mathbf{Q}_{\text{aug}}\mathbf{x}_{\text{aug}}(k) + \mathbf{u}^T(k)\mathbf{R}\mathbf{u}(k)),$$

where $\mathbf{Q}_{\text{aug}} = \text{diag}([\mathbf{Q}, \mathbf{Q}_p, \mathbf{Q}_r])$. The weighting matrices are given in Appendix A: \mathbf{R} – for control states, \mathbf{Q} – for physical plant states, \mathbf{Q}_p – for auxiliary states in the integral part, \mathbf{Q}_r – for auxiliary states in the oscillatory part.

The weighting matrices have been chosen assuming its diagonal structure. In order to produce the equal contribution to the cost function the Bryson's rule [26] has been applied. For weights collected in \mathbf{R} , \mathbf{Q} and \mathbf{Q}_p (see Appendix A) the r , q and q_p are divided by one because the control structure is already scaled to unity using measurement gain of the grid current and the control signals are in the range from -1 to 1. For the weights collected in \mathbf{Q}_r one of the two weights of the individual oscillatory term (9) is obtained using scaling by $(h\omega)^2$. The penalty weights q , q_p and q_{r2}, q_{r6}, q_{r12} are selected by trial-and-check method. The weights for the physical plant states (\mathbf{Q} matrix) and for the auxiliary states (\mathbf{Q}_p

and \mathbf{Q}_r matrices) are chosen using the rule of thumb saying that q should be several orders of magnitude smaller and $q_p, q_{r2}, q_{r6}, q_{r12}$ several orders of magnitude larger than r .

DC voltage controller design

An outer feedback control loop with PI regulator is used for the DC voltage stabilization. The regulator is tuned by the `system` Matlab's function [27] using linear average model of VSC. Before the tuning process the control design requirements must be specified. The `TuningGoal.Rejection` class [28] is used to specify the minimum attenuation profile expected at a point i_d^{ref} . The controller output value is kept within a feasible range, so the reference current is limited. The m-script with the `system` function call is given in Appendix B.

Simulation result - symmetrical grid voltage

The signal waveforms for the VSC operated under symmetrical grid voltage are presented in Fig. 4. in dq frame.

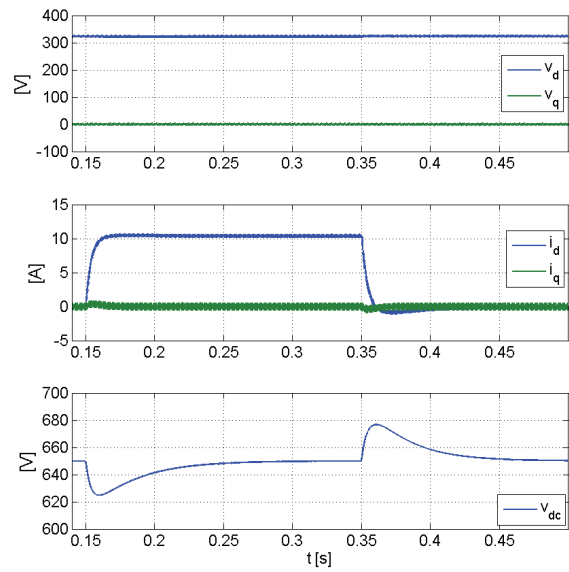


Fig. 4. Performance of the system with LQI current controller under 5 kW step of load from 0 to 100% and back to 0.

For this case only the proportional and the integral part of the current controller is used (LQI current control). The i_q^{ref} value is set to zero in order to ensure the unity power factor regulation. From the top: the grid voltage, the grid current and the DC-link voltage. The step of R_{load} from 0 to 100% occurs in 0.15 s and next back to 0 in 0.35 s. The i_d current is without overshoot after R_{load} is connected and about 1 A overshoot after R_{load} is disconnected. The tuned DC-link voltage controller provides 3% overshoot and settling time ca. 0.15 s on the DC-link voltage waveform.

Simulation results - distorted grid voltage

The simulated signal waveforms for the VSC operated under distorted grid voltage in the steady-state is presented in Fig. 5 to Fig. 7. From the top: the grid voltage, the grid current, the DC-link voltage. The grid voltage amplitude in the a phase is decreased by 15% in relation to the nominal value. The 5% of the 5th and 7th and the 3% of the 11th and 13th harmonic are added to the grid model. For each of the presented results the PLL is used [24]. The performance of the system in the steady-state under the distorted grid voltage conditions without enabling of the MOSC part is presented in the Fig. 5. In the next step, four oscillation terms, for $h = \{6, 12\}$ are applied to reduce the component

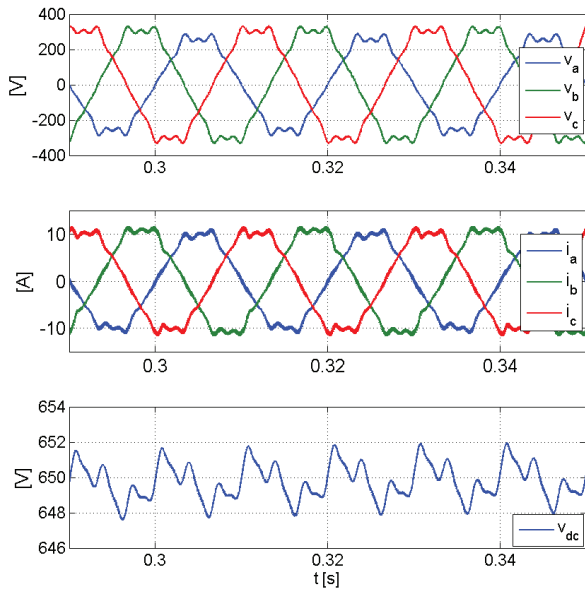


Fig. 5. Performance of the control system under distorted grid conditions with LQI current controller without MOSC part in steady-state.

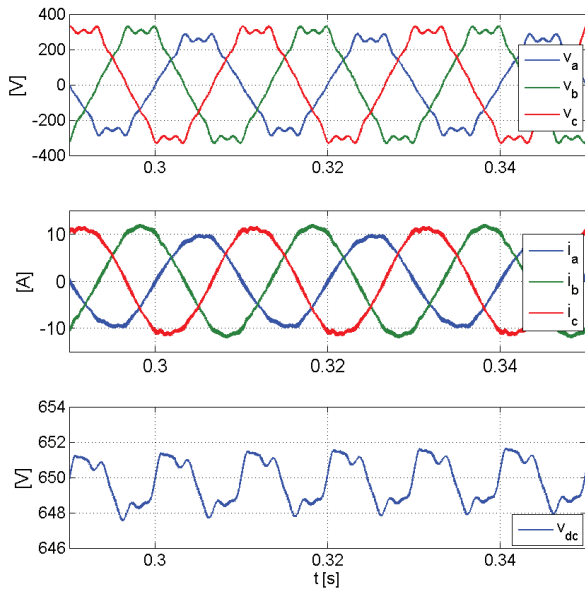


Fig. 6. Performance of the system under distorted grid conditions with LQI current control and MOSC part where $h = \{6, 12\}$ in steady-state.

of the pulsations 6ω and 12ω to zero in the error current signals after dq transformation. As a result, nearly sinusoidal grid currents are obtained as presented in Fig. 6.

In the next step, in order to obtain nearly symmetrical grid current, two new oscillation terms are added, so $h = \{2, 6, 12\}$. As a result, the symmetrical grid current is obtained as shown in Fig. 7. The value of the DC-link voltage oscillates because of the power fluctuation. The amplitude of this oscillation can be reduced by increasing capacitance of the DC-link. The DC-link voltage fluctuations are transmitted to the v_d^{ref} . However, in the case of up to approximately a dozen percent of the grid voltage unbalance, an additional attenuation of DC voltage oscillation is usually unnecessary. The selected model parameters used in simulations are presented in the Tab. 1.

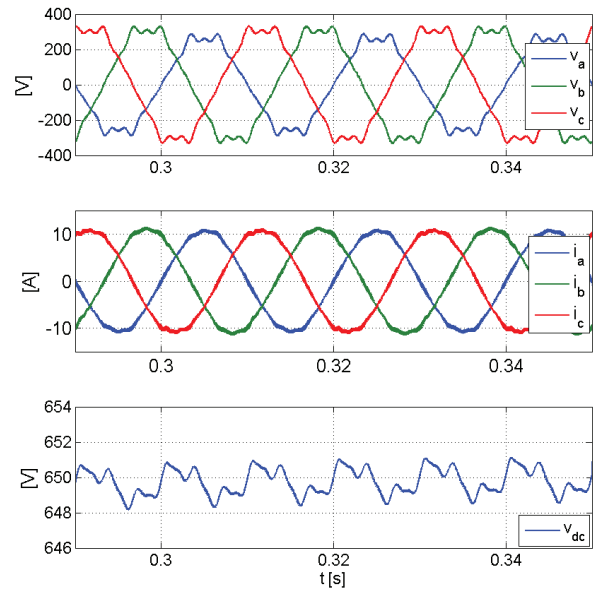


Fig. 7. Performance of the system under distorted grid conditions with LQI current control and MOSC part where $h = \{2, 6, 12\}$ in steady-state.

Table 1. Parameters of the simulation model

| Symbol | Value | Description |
|-----------------------|-------------------------|---------------------------------------|
| V_{dc} | 650 V | Nominal DC-link voltage |
| V_{dc}^{ref} | 1 V | Reference DC-link voltage |
| V | 325 V | Nominal phase-neutral grid voltage |
| ω | $100\pi \text{ s}^{-1}$ | Nominal pulsation of the grid voltage |
| L | 4.0 mH | Inductance of the input filter |
| R | 0.5 Ω | Resistance of the input filter |
| L_s | 0.1 mH | Inductance of the grid |
| R_s | 0.1 Ω | Resistance of the grid |
| C_{dc} | 1.0 mF | Capacitance of the DC-link capacitor |
| T_s | 0.0001 s | Switching/sampling time |
| R_{load} | 84 Ω | DC load parameter |
| k_i | $1/25 \text{ A}^{-1}$ | Measurement gain of the grid current |
| k_{dc} | $1/650 \text{ V}^{-1}$ | Measurement gain of DC-link voltage |
| - | continuous | Modulation type |

Conclusion

A full-state-feedback LQ current controller with the oscillatory terms for the grid-connected PWM converters operated under distorted grid conditions has been developed. The integral terms have been added to the input of the current controller to obtain a unity power factor. In order to obtain nearly sinusoidal symmetrical grid current under distorted grid voltage conditions the oscillatory terms are incorporated into the current control structure. The dynamic performance and steady-state behavior of the control system with the inner state current controller and the outer PI DC-link voltage controller have been verified in a simulation.

This study was co-financed from funds for statutory activity of Faculty of Electrical Engineering Warsaw University of Technology and from funds provided under a grant titled "Prostownik aktywny o sinusoidalnym prądzie wejściowym ze sterowaniem wykorzystującym sprzężenie od wektora stanu".

Appendix A

The weight matrices for (15):

$$\begin{aligned}
 \mathbf{R} &= \text{diag}\left(\left[\frac{r}{12}, \frac{r}{12}\right]\right), r = 1; \\
 \mathbf{Q} &= \text{diag}\left(\left[\frac{q}{12}, \frac{q}{12}\right]\right), q = 10^{-5}; \\
 \mathbf{Q}_p &= \text{diag}\left(\left[\frac{q_p}{12}, \frac{q_p}{12}\right]\right), q_p = 10^5; \\
 \mathbf{Q}_r &= \text{diag}\left(\left[\frac{q_{r2}}{12}, \frac{q_{r2}}{12}, \frac{q_{r2}}{(2\omega)^2}, \frac{q_{r2}}{(2\omega)^2}, \frac{q_{r6}}{12}, \frac{q_{r6}}{12}, \frac{q_{r6}}{(6\omega)^2}, \frac{q_{r6}}{(6\omega)^2}, \frac{q_{r12}}{12}, \frac{q_{r12}}{12}, \frac{q_{r12}}{(12\omega)^2}, \frac{q_{r12}}{(12\omega)^2}\right]\right), q_{r2} = 10^{10}, q_{r6} = 10^{12}, q_{r12} = 10^{14}
 \end{aligned}$$

Appendix B

M-script for the DC-link voltage controller tuning:

```
ST0=slTuner('Model','PI');
addPoint(ST0,'Id_ref');
s = tf('s');
Req = TuningGoal.Rejection('Id_ref',(s+100)/(s+0.1));
Options = systuneOptions('RandomStart',10);
systune
[ST1,fSoft,~,Info] = ST0.systune(Req,Options);
writeBlockValue(ST1);
% Model - name of the simulation model file.
% PI - name of the PI-type DC-link voltage regulator.
% Id_ref - name of the line-connected PI reg. output.
% Req - disturbance rejection requires at point Id_ref
% where (s+100)/(s+0.1) is assumed attenuation profile.
% Options - 10 randomized starting points for systune call.
% [ST1,fSoft,~,Info] - the systune output.
% writeBlockValue(ST1) - saving of the results to PI block.
```

REFERENCES

- [1] Malinowski M., Kazmierkowski M., Trzynadlowski A., A comparative study of control techniques for PWM rectifiers in AC adjustable speed drives, *IEEE Transaction on Power Electronics*, 18 (2003), n. 6, 1390–1396
- [2] Sedlak M., Stynski S., Kazmierkowski M.P., Malinowski M., Three-level four-leg flying capacitor converter for renewable energy sources, *Przegląd Elektrotechniczny (Electrical Review)*, 12a (2012), n. 2, 6–11
- [3] Pura P., Iwanski G., Direct Power Control of DFIG Connected to Unbalanced Power Grid, in proc. of *9th IEEE International Conference and Exhibition Ecological Vehicles and Renewable Energies (EVER)*, Monaco, 2013, 1–7
- [4] Benysek G., Kazmierkowski M.P. Popczyk J., Strzelecki R., Power electronic systems as a crucial part of Smart Grid infrastructure – a survey, *Bulletin of the Polish Academy of Sciences, Technical Sciences*, 59 (2011), n. 4, 455–473
- [5] Smolenski R., Jarnut M., Benysek G., Kempinski A., AC/DC/DC interfaces for V2G applications – EMC issues, *IEEE Transaction on Industrial Electronics*, 60 (2013), n. 3, 930–935
- [6] Kazmierkowski M.P., Krishnan R., Blaabjerg F., Kempinski A., Control in Power Electronics, Selected Problem *Academic Press*, London, UK, 2002
- [7] Alepuz S., Busquets-Monge S., Bordonau J., Martinez-Velasco J.A., Silva C. A., Pontt J. and Rodriguez J., Control strategies based on symmetrical components for grid-connected converters under voltage dips, *IEEE Transaction on Industrial Electronics*, 56 (2009), n. 6, 2162–2173
- [8] Kazmierkowski M.P., Jasinski M., Wrona G., DSP-Based Control of Grid-Connected Power Converters Operating Under Grid Distortions, *IEEE Transaction on Industrial Informatics*, 7 (2011), n. 2, 204–211
- [9] Piasecki S., Jasiński M., Rafał K., Korzeniewski M., Milicua A., Higher harmonics compensation in grid-connected PWM converters for renewable energy interface and active filtering, *Przegląd Elektrotechniczny*, 6 (2011), 85–90
- [10] Barote L., and Marinescu C., Teodorescu R., Current controller considering harmonics compensation for grid connected converter in DPGS applications, in proc. of *13th IEEE Conference on Optimization of Electrical and Electronic Equipment (OPTIM)*, Romania, 2012, 899–905
- [11] Rodriguez J., Kazmierkowski M.P., Espinoza J.R., Zanchetta P., Abu-Rub H., Young H.A., Rojas C.A., State of the Art of Finite Control Set Model Predictive Control in Power Electronics, *IEEE Trans. on Industrial Infor.*, 9 (2013), n. 2, 1003–1016
- [12] Wojciechowski D., Strzelecki R., Predictive control of active filter system with LCL coupling circuit, in proc. of *9th IEEE International Power Energy Conference (IPEC)*, Singapore, 2010, 2276–2282
- [13] Dannehl J., Fuchs F.W., Flatness-based voltage-oriented control of three-phase PWM rectifiers, in proc. of *13th IEEE International Power Electronics and Motion Control Conference (EPE-PEMC)*, Poland, 2008, 444–450
- [14] Zhixiang Zou, Zheng Wang, Ming Cheng, Yongheng Yang, Active power filter for harmonic compensation using a digital dual-mode-structure repetitive control approach, in *3rd IEEE International Symposium on Power Electronics for Distributed Generation Systems (PEDG)*, Denmark, 2012, 161–166
- [15] Dannehl J., Fuchs F.W., Thogersen P.B., PI State Space Current Control of Grid-Connected PWM Converters With LCL Filters, *IEEE Trans. on Power Electr.*, 25 (2010), n. 9, 2320–2330
- [16] Pena-Alzola R., Liserre M., Blaabjerg F., Sebastian R., Dannehl J., Fuchs F.W., Systematic Design of the Lead-Lag Network Method for Active Damping in LCL-Filter Based Three Phase Converters, *IEEE Transaction on Industrial Informatics*, 10 (2014), n. 1, 43–52
- [17] Kedjar B., Kanaan H.Y., Al-Haddad K., Vienna Rectifier With Power Quality Added Function, *IEEE Transaction on Industrial Electronics*, 61 (2014), n. 8, 3847–3856
- [18] Kedjar B., Al-Haddad K., LQR with Integral Action to Enhance Dynamic Performance of Three-Phase Three-Wire Shunt Active Filter, in proc. of *IEE Power Electronics Specialists Conference (PESC)*, USA, 2007, 1138–1144
- [19] Kaszewski A., Ufnalski B., Grzesiak L.M., An LQ controller with disturbance feedforward for the 3-phase 4-leg true sine wave inverter, in proc. of *6th IEEE International Conference on Industrial Technology (ICIT)*, 2013, 1924–1930
- [20] Kaszewski A., Ufnalski B., Grzesiak L.M., The LQ controller for the 3-phase 4-leg inverter with an LC output filter – Choosing the right reference frame, in proc. of *15th European Conference on Power Electronics and Applications (EPE)*, South Africa, 2013, 1–9
- [21] Ufnalski B., Kaszewski A., Grzesiak L., Particle Swarm Optimization of the Multi-oscillatory LQR for a 3-phase 4-wire Voltage Source Inverter with an LC Output Filter, *IEEE Transaction on Industrial Electronics*, 2014, 1–10
- [22] Alepuz S., Busquets S., Bordonau J., Pontt J., Silva C., Rodriguez J., Balanced grid currents in three-level voltage-source inverters connected to the utility under distorted condition using symmetrical components and linear quadratic regulator, in proc. of *12th European Conference of Power Electronics and Applications (EPE)*, Denmark, 2007, 1–10, 2007
- [23] Eloy-Garcia J., Arnaltes S., Rodriguez-Amenedo J.L., Direct power control of voltage source inverters with unbalanced grid voltages, *IET Power Electronics*, 1 (2008), 395–407
- [24] Marques G.D., Pires V.F., Malinowski M., Kazmierkowski M., An Improved Synchronous Reference Frame Method for Active Filters, in proc. of *International Conference on "Computer as a Tool" (EUROCON)*, Poland, 2007, 2564–2569
- [25] Kanaan H.Y., and Hayek A., and Al-Haddad K., Small-Signal Average Modeling, Simulation and Carrier-Based Linear Control of a Three-Phase Four-Leg Shunt Active Power Filter, in proc. of *IEEE International Electric Machines Drives Conference (IEMDC)*, Turkey, 1 (2007), 601–607
- [26] Franklin G., Powell D., Workman M., *Digital Control of Dynamic Systems* (3rd Edition), *Prentice Hall*, 1997
- [27] www.mathworks.com/help/robust/gs/tuning-control-systems-with-systune.html, Tuning Control Systems with SYSTUNE, *MathWorks Documentation Center*, (18.07.2014)
- [28] www.mathworks.com/help/robust/gs/pid-tuning-for-setpoint-tracking-vs-disturbance-rejection.html, PID Tuning for Setpoint Tracking vs. Disturbance Rejection, *MathWorks Documentation Center*, (18.07.2014)

Authors: mgr inż. Andrzej Galecki, dr inż. Arkadiusz Kaszewski, prof. dr hab. inż. Lech M. Grzesiak, dr inż. Bartłomiej Ufnalski, Institute of Control and Industrial Electronics, Faculty of Electrical Engineering, Warsaw University of Technology, ul. Koszykowa 75, 00-662 Warszawa, Poland, email: andrzej.galecki@ee.pw.edu.pl